Spectrum sliced wavelength division multiplexing based free space optical communication employing differential quadrature phase shift keying and optical frequency comb generation

NAGA SUBRAHMANYA VAMSI MOHAN YARRA[1,*], A. SIVANANTHA RAJA[1], K. ESAKKI MUTHU[2]
[1]Department of Electronics and Communication Engineering, Alagappa Chettiar Government College of Engineering and Technology, Karaikudi, Tamilnadu, India
[2]Department of Electronics and Communication Engineering, University College of Engineering, Anna University Regional Campus, Madurai, Tamilnadu, India

A spectrum-sliced (SS) Wavelength division multiplexing (WDM) based Free-space optical (FSO) communication system at a data rate of 5x32 Gbps is proposed in this research article. Based on the concept of Optical Frequency Comb Generator (OFCG), the optical spectrum is sliced into 32 parts so that the data rate is improved by 32 times. A cost-efficient, 160 Gbps WDM FSO system is designed and implemented using the Opti-system software. In WDM, multiple lasers are needed. Hence, the price of the system increases. To reduce cost, an optical multicarrier generation system is required. The proposed system design generates multiple wavelengths, thereby splitting the available spectrum into 32 channels with a fixed channel spacing of 25 GHz. The produced optical comb has a width of 10 nm, starting from a wavelength of 1544.8 nm to 1555.2 nm. The proposed work reveals that the differential quadrature phase shift keying (DQPSK) based SS-WDM FSO system has higher performance compared to intensity modulation formats and other differential phase modulation formats. Considering various values of FSO link distances, antenna diameters of transmitter and receiver, beam divergence and, thus determining the values of performance metrics such as Q-factor and bit error rate (BER), the DQPSK-based SS-WDM FSO system is simulated.

1. Introduction

Optical wireless communication systems are broadly divided into indoor and outdoor systems. Outdoor systems are also known as free space optical (FSO) systems. The very first implementation of a free space optical (FSO) communications link was demonstrated by Alexander Graham Bell on 3rd June, 1880 with his new invention known as photophone [1]. The photophone is a device that allows the transmission of sound on a light beam. FSO communication is line of sight (LOS) communication with a light source such as a continuous wave (CW) laser and a photodetector to detect light transmitted through free space. Here, the operating frequency of the CW laser will be in the tera hertz range. The receiver section includes a low-pass filter that eliminates the noise generated during the transmission through the free space channel. Since the light beams are transmitted through free space, no fiber optic cable is required. The advantages of FSO include enormous modulation bandwidth, low cost of deployment, unlicensed spectrum, no electromagnetic interference (EMI) and, fast deployment time [2].

Each WDM channel used for FSO requires a light source. Therefore, the need for multiple light sources increases the cost of the FSO system. Spectrum-sliced WDM drastically reduces this cost. SS-WDM was investigated by non-return to zero (NRZ) format at a data rate of 2.5 Gbit/s [3]. Semiconductor optical amplifiers (SOA), light emitting diodes (LEDs), highly nonlinear fibers (HNLF), and arrayed waveguide gratings (AWG) are various components for spectrum slicing [4]. Optical comb can produce spectrum slicing at a reduced cost [5]. An optical comb can be expanded to 128 coherent lines [6].

An optical frequency comb (OFC) is a uniformly spaced set of discrete optical frequencies. OFCs have a wide range of applications in various fields such as optical communication (to increase the capacity and spectral efficiency of optical networks), metrology (as a ruler for measuring optical frequencies with high precision) and, spectroscopy (to enable high-precision, high-speed measurements of gas concentrations) [7]. OFCs can be realized using various techniques, such as femto second mode-locked lasers (MLL) [8], exploiting third-order nonlinearity in nonlinear optical mediums [9], resonant structures [10] and electro-optic modulator-based [11] approaches. MLL lasers generate a train of ultra-short pulses with a well-defined repetition rate, which corresponds to the mode spacing of the frequency comb. The discrete frequencies in the pulses' optical spectrum are spaced according to the pulse repetition rate. There are limitations of traditional MLL-based OFC generation techniques such as limited line spacing, less stability, high complexity, and controllability issues [12]. MLL lasers

offer high power and broad bandwidth, but they can be bulky and expensive.

A micro-resonator is made up of a tiny cavity that can support high-quality-factor (Q) optical modes. Light can circulate several times in a cavity when a narrowband laser is linked to it, creating a comb of optical frequencies that are equally spaced. This approach has been demonstrated using various materials, including silicon [13], silica, and diamond. Micro-resonators offer compactness and low power consumption, but they can be challenging to fabricate and have lower power output. The Optical Frequency Comb (OFC) can be generated using third-order nonlinearity in nonlinear optical mediums or resonant structures through four-wave mixing (FWM). This process produces output waves with frequencies equal to the sum and difference of input frequencies, resulting in an OFC [14] with a comb-like spectrum. A fourth approach for OFC generation is based on electro-optic modulation. This technique creates a train of optical pulses with a predetermined repetition rate using an electro-optic modulator and a continuous-wave laser. The discrete frequencies in the pulses' optical spectrum are spaced according to the pulse repetition rate. This method has been shown with various materials, such as gallium arsenide and lithium niobate. Electro-optic modulation offers simplicity and flexibility, but it can have lower spectral purity and stability.

SS-FSO system demonstrated for an FSO communication distance of over 2.5 km [15]. SS-WDM-FSO system with up to 16 channels and effects of turbulence due to various factors such as buildings' height and the wind speed reported [16]. SS-WDM-FSO was demonstrated with an advanced modulation format such as carrier-suppressed return to zero (CSRZ), and various line coding techniques [17]. The line coding techniques implemented are return to zero (RZ), and non-return to zero (NRZ). For amplification of the signal in the SS-WDM-FSO system, the performance of various amplifiers such as Raman amplifiers, semiconductor optical amplifiers, and erbium-doped fiber amplifiers (EDFA) were investigated and reported that eye-opening of the SS-WDM system using the latter is the best compared to the rest of the amplifiers[18].SS-WDM with 10Gbits/s power efficient advanced modulation format, modified duo binary return to zero (MDRZ) for the downlink and OOK (on-off keying) non-return to zero(NRZ) for the uplink was proposed [19].

In addition to spectral slicing, there are a number of factors that determine the overall performance of the SS-WDM-FSO system such as the distance of the FSO link (km), the beam divergence angle (mrad) and the antenna diameters of the transmitter as well as receiver (cm) [20]. A comparison of FSO with SS-WDM and without SS-WDM for various weather conditions using NRZ modulation format was reported and showed that SS-WDM provides better performance for different weather conditions [21]. SS-WDM has been compared with Spectrum Amplitude Coding (SAC) Optical Code Division Multiple Access (Optical CDMA) systems for different light sources [22]. The above research work shows that when compared to Optical CDMA, SS-WDM provides more spectral efficiency because of no necessity for bandwidth expansion. Many researchers provided several methods for the improvement of FSO links' overall performance in terms of performance metrics such as BER and Q-factor. Strhel ratio (SR) and BER are used to analyze the performance of FSO link [23].

A hybrid version of SS-WDM combined with Polarization division multiplexing (PDM) is proposed to enhance the performance of FSO system [24]. A hybrid SSWDM FSO system implementing orthogonal frequency division multiplexing (OFDM) and Mode division multiplexing utilizing Hermite Gaussian modes has been proposed to increase the link distance under clear weather conditions, and different fog conditions to achieve a data rate of 160 Gbps [25]. A hybrid SSWDM FSO system implementing orthogonal frequency division multiplexing (OFDM) and Mode division multiplexing utilizing Laugerre Gaussian modes has been proposed to increase the link distance under clear weather conditions [26], and different fog conditions to achieve a data rate of 160 Gbps [27]. For the mitigation of atmospheric effects, an SS-WDM system is implemented using pre-amplification and post-amplification [28]. Mitigation of severe scintillation effects are demonstrated [29] by means of a spectrum sliced light source with reflective semiconductor optical amplifiers (RSOAs).A high-speed long-distance FSO link with hybrid 16-QAM-PDM was proposed for the implementation of 5G-enabledInternet of Things (IoT) [30].

There is still scope for the betterment of FSO links' overall performance and spectrum utilization. Hence, in this research work, an FSO system by cost effective spectral slicing WDM (SS-WDM) with a data rate of 5x32 Gbps using optical comb and DQPSK modulation is proposed. Simulation of the SS-WDM-FSO system based on DQPSK is performed at various beam divergence angles, FSO link distances and transmitter as well as receiver-antenna diameters in terms of Q-factor and BER.

The DQPSK modulation scheme encodes two bits per symbol. This doubles the utilization of the spectrum. Using DQPSK, the symbol rate is halved, for the same bit rate. This improves tolerance to dispersion and nonlinearities [31-32]. SS-WDM system is investigated for clear weather, fog, different rain conditions and haze [33]. SS-WDM may be developed by means of amplified spontaneous emission (ASE) noise for SOA [34,35].

2. Structure of the system model

Using the well-known Opti-system simulation tool, the proposed SS-WDM-FSO system with DQPSK modulation is implemented. Fig. 1 shows the block diagram of the SS-WDM-FSO communication system. The architecture [36] to produce the optical frequency comb contains a continuous wave (CW) laser at a wavelength of 1550 nm, which provides an input power of 30 dBm. The signal from the CW laser source is fed to a dual port optical spectrum analyzer.
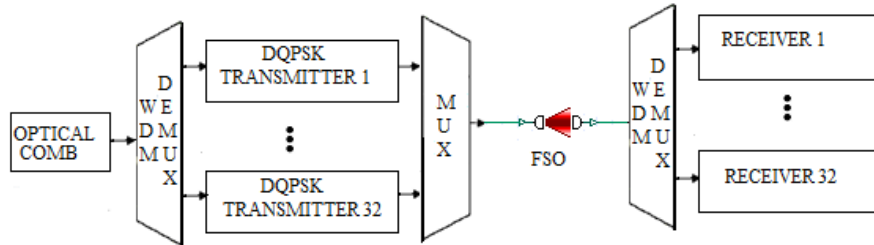
Fig.1.Block diagram of SS-WDM-FSO system employing optical comb and DQPSK

Table 1. Turbulence regimes [5]

C_n^2 (m$^{-2/3}$)	Turbulence regimes		
	Weak	Moderate	Strong
	5×10^{-16}	5×10^{-14}	5×10^{-12}

Table 2. System parameters for the research work

S. No.	Parameter	Values
1	CW laser frequency	193.414 THz
2	CW Laser Power	30 dBm
3	Spectrum-sliced WDM Channels	32
4	Frequency spacing	25 GHz
5	FSO link distance	1-9 km
6	Beam divergence	0.25, 0.50, 0.75 and 1 mrad
7	Transmitter/Receiver antenna diameters	5, 10, 15 and 20 cm
8	Attenuation for clear weather	0.1 dB/km [17]
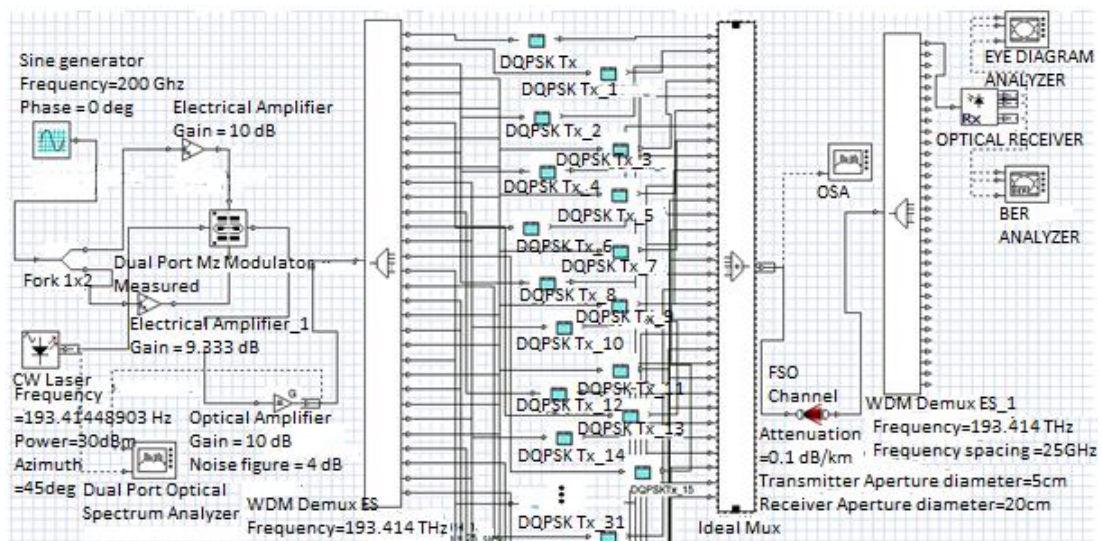
Fig. 2. (a). Proposed simulation model for SS-WDM-FSO employing DQPSK (color online)

Proposed system parameters are shown in Table 2 for the DQPSK modulated SS-WDM-FSO system. The simulation model of the SS-WDM-FSO system incorporating DQPSK is shown in Fig. 2(a). Fig. 2(b) displays DQPSK Transmitter. A sine generator at a frequency of 200 GHz and phase 0 degrees is fed to a 1x2 fork, so that the signal is divided into two routes. The signals from both routes get amplified by two electrical amplifiers, one with a gain of 10 dB, second one with a gain of 9.333 dB, which are fed to dual port Mach Zehnder Modulator (MZM). The OFCG is connected to a WDM-Demultiplexer, which splits the optical spectrum into individual channels. 32 flat channels are generated with a spacing of 25 GHz. Each distinct channel is modulated by means of DQPSK modulation. All the modulated channels are combined using multiplexer to be transmitted via the FSO channel. Each distinct channel is detected by means of individual optical receivers consisting of a PIN photodiode, low pass filter and 3R regenerator. The spectrum is sliced into 32 equally spaced optical channels. The proposed Opti-system layout for SS-WDM-FSO is shown in Fig. 2(a). Pseudorandom bit sequence generators generate random data which is fed to DQPSK transmitters. The DQPSK transmitter diagram is shown in Fig. 2(b).
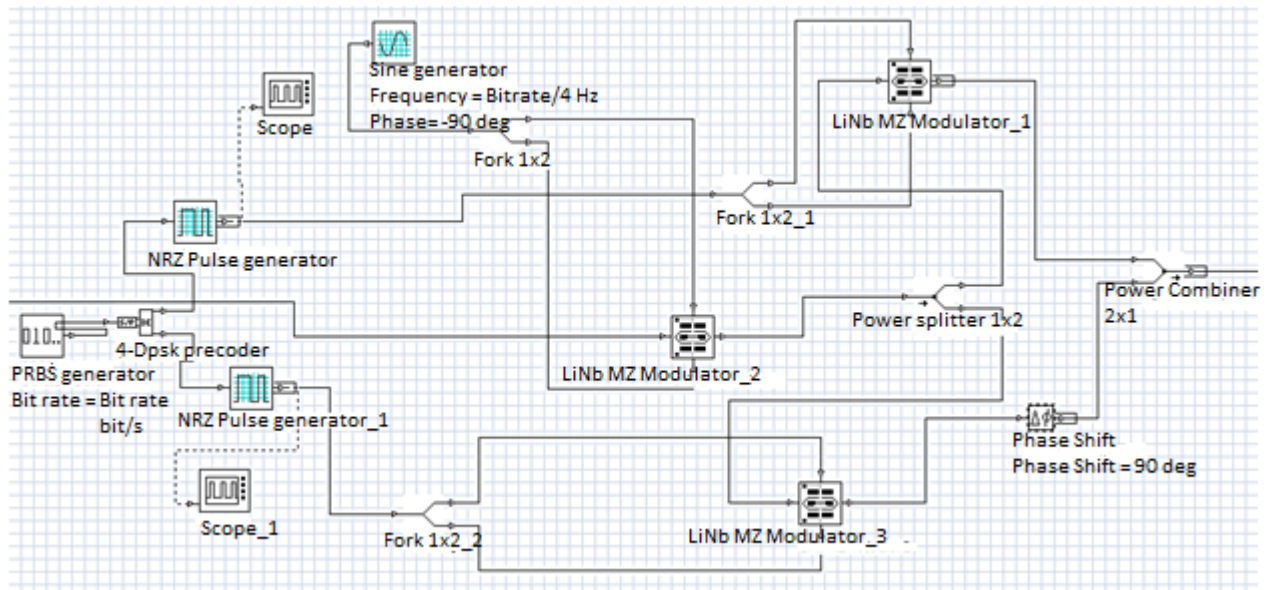
Fig. 2. (b)DQPSK Transmitter (color online)

Each DQPSK transmitter has a pseudorandom bit sequence generator, a 4-dpsk pre-coder, two non-return to zero (NRZ) pulse generators, a sine generator and three MZMs. The sliced signals are multiplexed after the modulation. The multiplexed signals are transmitted from the transmit antenna to the receive antenna towards the receiver via free space. The received data signals are reconstructed back to the original stream of data. In clear weather conditions, the FSO system suffers from atmospheric turbulence. This turbulence is assumed to be between weak and moderate. Hence Refractive index structure parameter is assumed as $C_n^2 = 5 \times 10^{-15} m^{-2/3}$. Values of C_n^2 are shown in Table 1 [5]. Gamma-Gamma model is considered for this research work.

Fig. 3 shows the optical spectrum slices at the dual port optical spectrum analyzer.
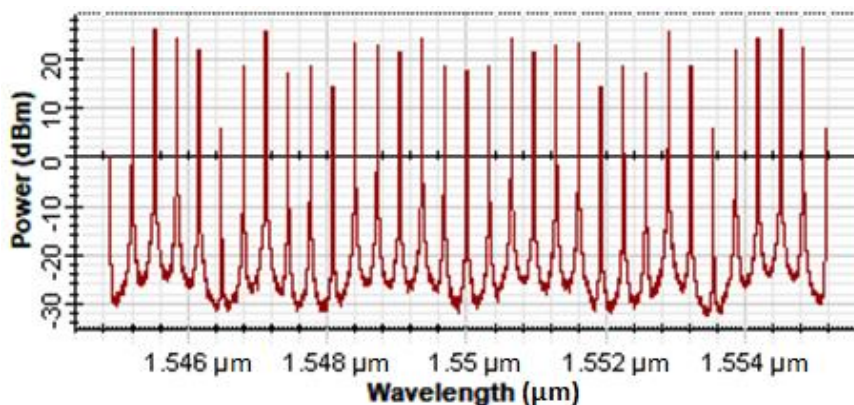
Fig.3.Optical spectrum slices at the dual port optical spectrum analyzer (color online)

3. Results and discussion

Different intensity modulation formats such as RZ, NRZ, and CSRZ are simulated using HNLF of 2 km length [20], and it is found that CSRZ has the best Q-factor considering all three intensity modulation formats. The differential phase modulation format DPSK has been reported using HNLF of 2 km length [37] and it was found that DPSK outperforms intensity modulation formats. Therefore, in the proposed SS-WDM-FSO system, another differential phase modulation technique DQPSK, is investigated and a comparison is made with both the intensity modulation formats [20] and DPSK format [37] as shown in Fig. 4.

To study the performance of the high-speed SS-WDM-FSO communication system, various factors such as the distance of the FSO link, the divergence angle of the beam, different modulation formats, and the diameters of the transmit and receive antennas are considered. To investigate the quality of signal reception, the length of the FSO link is varied from 1 km to 5 km. The simulation shows that the quality of the received signal deteriorates as the link length increases. Different modulation formats have different values of the Q factor. A suitable modulation format must be investigated where the performance degradation is the smallest. The SS-WDM-FSO link performance in terms of Q-factor is shown in Table 3 for DQPSK, DPSK, CSRZ, NRZ, and RZ. Fig. 4 shows the Q-factor performance (vs) link range of the SS-WDM-FSO link for different modulation formats. The Q-factor varies from 23.49 to 14.02 for DQPSK, 22.96 to 11.78 for DPSK 15.20 to 9.57 for CSRZ, 14.16 to 9.44 for NRZ, and 12.86 to 9.13for RZ for an FSO link range of 1 to 5 km under clear weather.

Table 3. Values of Q-factor at various link distances for different modulation formats

Link distance (km)	Q-factor				
	DQPSK	DPSK	CS-RZ	NRZ	RZ
1	23.49	22.96	15.20	14.16	12.86
2	21.42	19.97	14.56	13.91	12.86
3	19.11	17.02	13.34	12.69	12.01
4	16.63	14.24	11.54	11.44	11.23
5	14.02	11.78	9.57	9.44	9.13

Table 4. Values of log (BER) at various link distances

Link distance(km)	Log (BER)				
	DQPSK	DPSK	CS-RZ	NRZ	RZ
1	-122	-117	-52	-46	-44
2	-101	-89	-50	-45	-39
3	-81	-65	-46	-42	-36
4	-62	-46	-38	-37	-36
5	-44	-32	-26	-25	-22
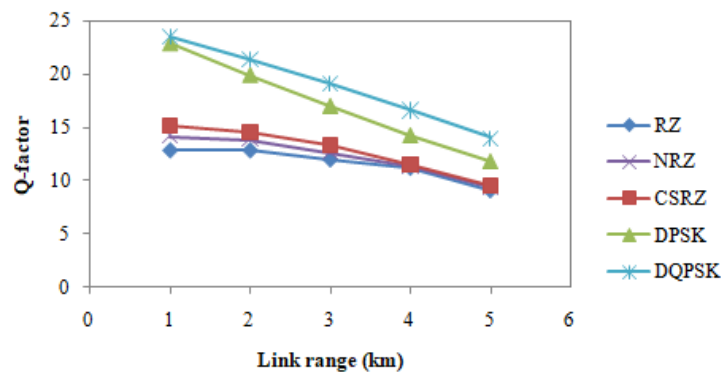
Fig. 4. Graph of Q-factor (vs) distance (km) (color online)
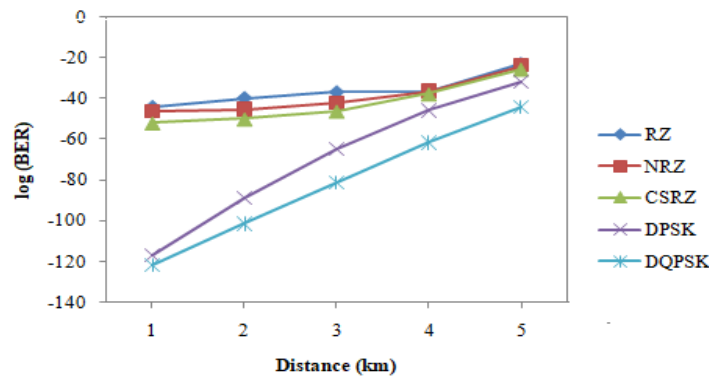
Fig. 5. Graph of log (BER) (vs) link distance (km) (color online)
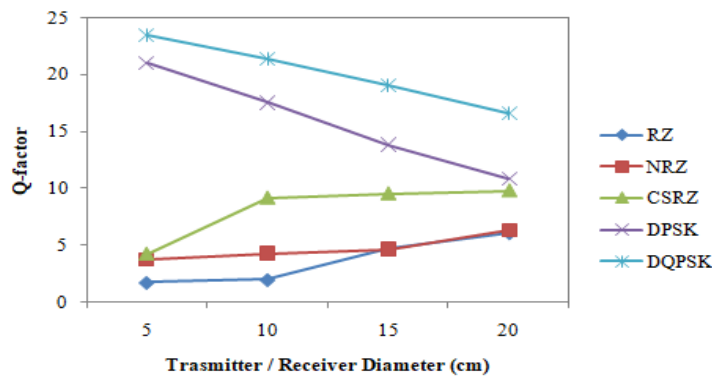
Fig.6. Graph of Q-factor (vs) Transmitter/Receiver diameter (cm) (color online)
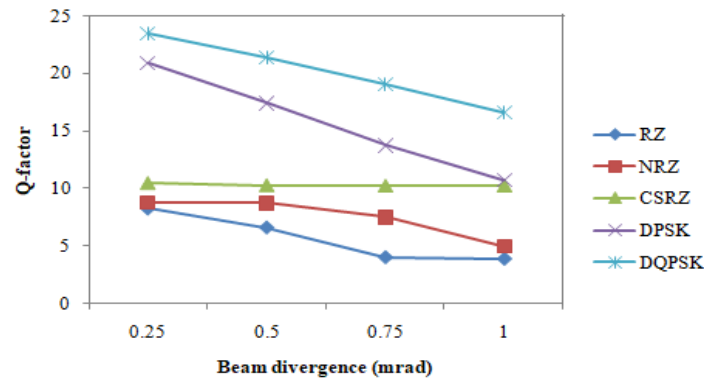
Fig.7. Graph of Q-factor (vs) beam divergence (color online)

Different modulation schemes were tested to investigate the system performance. As shown in Fig. 4, DQPSK achieves the highest Q-factor. Table 4 shows the values of log (BER) with link distances up to 5 km for DQPSK, DPSK, CSRZ, NRZ and RZ modulation schemes. It is found that DQPSK outperforms both DPSK and various intensity modulation formats because this modulation scheme can suppress nonlinear effects to a significant extent, has higher spectral effectiveness, and has good tolerance to polarization mode dispersion and chromatic dispersion. A transmission distance of 9 km is achieved for SS-WDM-FSO employing DQPSK. Next to DQPSK is DPSK, followed by CSRZ, NRZ and RZ. Fig.5 shows a graph of log (BER) (vs) SS-WDM-FSO link distance for different modulation formats, from -122 to -44 for DQPSK, -117 to -32 for DPSK, -52 to -26 for CSRZ, -46 to -25 for NRZ and -44 to -22 respectively for RZ with FSO link distances from 1 to 5 km. There is an increase in log (BER) value, once the link distance is increased. Minimum bit errors are noticed in the case of DQPSK, followed by DPSK.

The performance analysis of the proposed SS-WDM-FSO system is studied in terms of Q-factor by increasing the diameter of the transmit/receive aperture from 5 to 20 cm in 5cm increments under clear weather conditions as shown in Fig. 6. By increasing the receiver aperture diameter, an improvement in the Q-factor can be observed because a larger receiver aperture diameter couples more power from the transmitter to the receiver. Therefore, the maximum power is received when the receiver aperture

diameter is 20 cm. With further investigation, the beam divergence angle is increased in steps of 0.25 mrad, 0.5 mrad, 0.75 mrad, and 1 mrad. As shown in Fig. 7, the maximum Q-factor is reached at the divergence angle of 0.25 mrad and the minimum at 1 mrad. BER of the received signal increases as the beam divergence angle increases and the Q-factor deteriorates.

Eye-diagrams of the investigated system at different link distances of 1 km to 5 km are displayed in Figs. 8 (a),

(b), (c), (d) and (e) respectively for SS-WDM-FSO employing DQPSK. The Eye-opening height of the proposed SS-WDM-FSO system reduces with the increase of the link distance. At 1 km link separation, clear eye-opening is noticed and a decrease in eye-opening height is seen at 5 km.

Table 5 shows the comparison in terms of results for the proposed research work with other existing works.
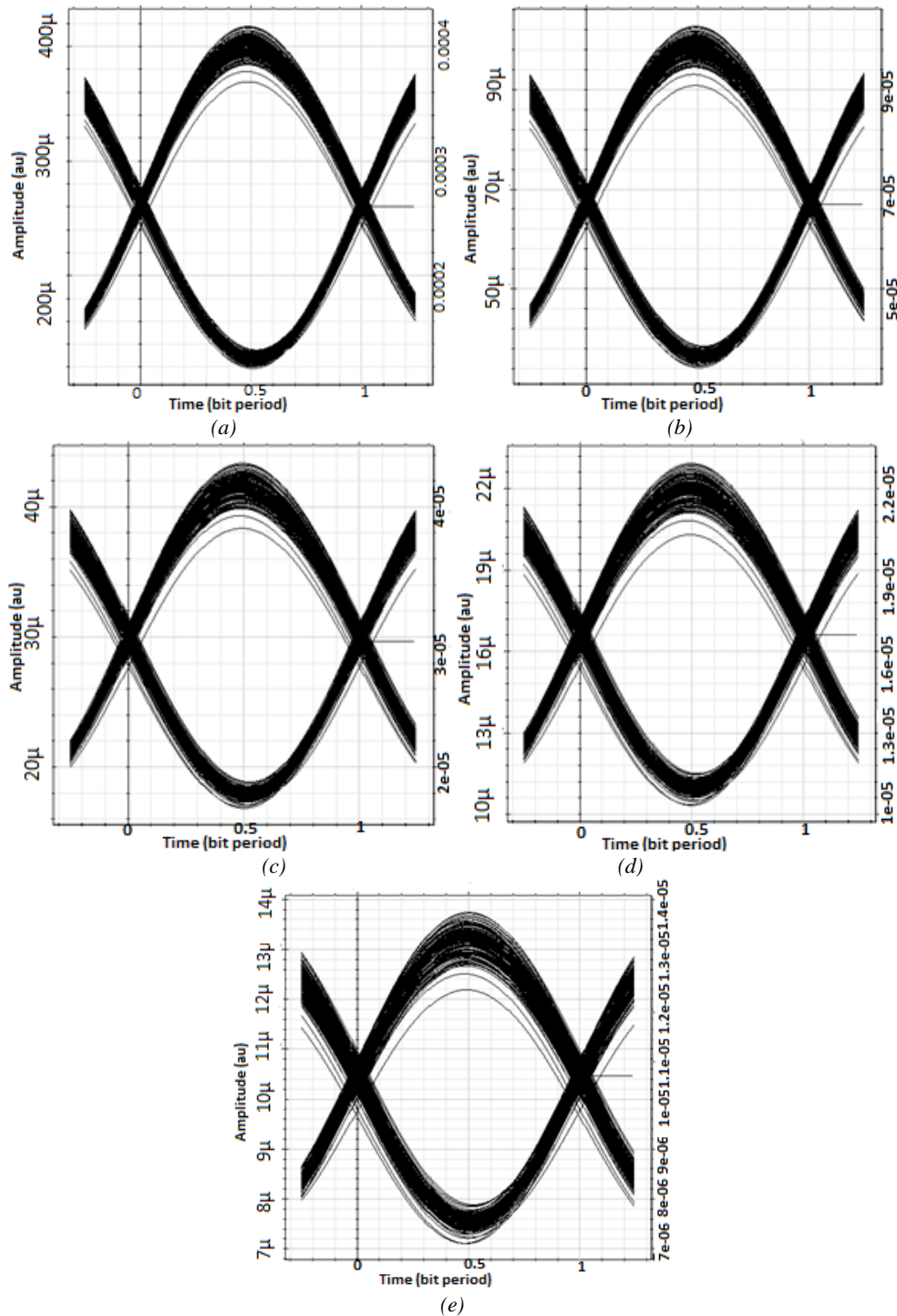
Fig. 8. Eye diagrams of SS-FSO at (a)1 km, (b)2 km, (c)3 km, (d)4 km, (e)5 km

Table 5. Comparison of results for the proposed research work with other existing works

Work / Author	Technique Used for Spectral slicing	Modulation Scheme	Data Rate	Maximum Transmission Distance	Maximum Q-factor	Minimum Log (BER)
A. Thakur et al. [20]	HNLF & Demux	CSRZ	10 Gbps	5 km	15.20	-52
A. Grover et al. [26]	HNLF & Demux	4-QAM	160 Gbps	20 km	-	-
A. Grover et al. [25]	HNLF & Demux	4-QAM	160 Gbps	30 km	-	-
P. Ravesh et al. [37]	HNLF & Demux	DPSK	10 Gbps	10 km	22.96	-117
Proposed Work	OFCG & Demux	DQPSK	160 Gbps	9 km	23.49	-122

4. Conclusion

In this research, a spectrum-sliced WDM-OFCG-FSO communication system with 32 uniformly distributed optical channels at a data rate of 5 Gbps each is investigated. The performance of the proposed SS-WDM-FSO system integrated with DQPSK is compared in terms of Q-factor, log(BER) at different values of transmitter/receiver antenna aperture diameters, beam divergence angles, and link spacing with different modulation formats such as NRZ, RZ and CSRZ. The results show that DQPSK performs better than DPSK, CSRZ, NRZ and RZ in terms of Q-factor and BER. This is because DQPSK can suppress nonlinear effects to a significant extent, has higher spectral effectiveness, and hasa good tolerance to polarization mode dispersion and chromatic dispersion. A transmission distance of 9 km and data rate of 160 Gbps is achieved. Future work to investigate advanced modulation formats such as Binary phase-shift keying (BPSK) and Offset quadrature phase-shift keying (OQPSK) can be considered.

References

[1] A. G. Bell, The Electrician **5**, 220 (1880).

[2] Z. Ghassemlooy, P. W. Oyewole, Mobile and Wireless Communications, eds. S. A. Fares, F. Adachi Rijeka, IntechOpen, 355 (2010).

[3] Ahmed, Nasim, Aljunid, S. Alwee, Ahmad, R. Badlisha, Fadil, H. Adnan, M. A. Rashid, Journal of Optical Communications **32**, 137 (2011).

[4] J. Jindal, A. Kumar, R. Kumar, International Conference on Integrated Interdisciplinary Innovations in Engineering **1033**, 012074 (2021).

[5] J. Mirza, W. A. Imtiaz, A. J. Aljohani, A. Atieh, S. Ghafoor, Alexandria Engineering Journal **59**, 4621 (2020)

[6] Q. Dong, B. Sun, F. Chen, J. Jiang, Photonic Sensors **6**, 85(2016).

[7] I. Coddington, N. Newbury, W. Swann, Optica **3**, 414(2016).

[8] Y.-J. Kim, J. Jin, Y. Kim, S. Hyun, S.-W. Kim, Optics Express **16**, 264 (2008).

[9] S. Vishal, S. Surinder, G. B. Lovkesh, A. A. Elena, V. A. Alexey, Optical Engineering **60**, 066108 (2021).

[10] P. Del'Haye, A. Schliesser, O. Arcizet, T. Wilken, R. Holzwarth, T. J. Kippenberg, Nature Photonics **450**, 1214 (2007).

[11] P. Martin-Mateos, A. Porro, P. Acedo, IEEE Photonics Technology Letters **30**, 161 (2018).

[12] Y. Siyuan, B. Fangdi, H. Hao, IEEE Photonics Journal **10**, 1 (2018).

[13] J. Pfeifle, V. Brasch, M. Lauermann, Nature Photonics **8**, 375 (2014).

[14] T. Herr, V. Brasch, J. D. Jost, C. Y. Wang, N. Kondratiev, M. L. Gorodetsky, T. J. Kippenberg, Nature Photonics **8**, 145 (2013).

[15] F. Rashidia, J. He., L. Chena, Optics Commun. **387**, 296(2017).

[16] K. Prabu, S. Charanya, M. Jain, D. Guha, Optics Communications **403**, 73 (2017).

[17] A. Thakur, S. Nagpal, A. Gupta, Wireless Pers. Commun. **100**, 1775 (2018).

[18] A. Thakur, S. Nagpal, Journal of Optical Communications **41**, 9 (2018).

[19] S. Magidi, A. Jabeena, Journal of Optical Communications **44**, 271 (2019).

[20] A. Thakur, A. Gupta, H. Singh, S. Bakshi, R. Goyal, G.Singh, N. Mohan, A. Singhal, Opt. Quantum Electron. **6**,53 (2021).

[21] E. Vasani, V. Sha, Opt. Rev. **29**, 383 (2022).

[22] H. A. Fadhil, T. H. Abd, H. M. R. Al-Khafaji, S. A. Aljunid, International Journal of Electrical, Computer, Energetic, Electronic and Communication Engineering **6**, 4 (2012).

[23] T. Pasupathi, J. A. V. Selvi, Proc. Natl. Acad. Sci. India, Sect. A Phys. Sci. **92**, 659 (2021).

[24] E. Vasani, V. Sha, Wireless Personal Commun. **130**, 777 (2023).

[25] A. Grover, A. Sheetal, Optoelectron. Adv. Mat. **14**(3-4), 136 (2020).

[26] A. Grover, A. Sheetal, Wireless Personal Commun. **125**, 2737 (2022).

[27] A. Grover, A. Sheetal, Trans. Emerging Tel. Tech. **31**(6), 3897 (2020).

[28] D. Aurora, H. S. Saini, J. Kaur, Optical and Quantum Electronics **54**,258 (2022).

[29] D. Lee, V. V. Mai, H. Kim, IEEE Photonics Technology Letters **33**(5), 227 (2021).

[30] V. Dhasarathan, M. Singh, J. Malhotra, Wireless Networks **26**(4), 2403 (2020).

[31] T. Tokle, C. R. Davidson, M. Nissov, J. X. Cai, D. Foursa, A. Pilipetski, IEEE Electron Lett. **40**, 444 (2004).

[32] L. Sharan, Agrawal, M. Vaibhav, V. K. Chaubey,

Journal of Optical Communications **38**, 297 (2017).

[33] G. Sharma, L. Tharani, 2nd International Conference on Micro-Electronics and Telecommunication Engineering (ICMETE), Ghaziabad, India, 210 (2018).

[34] K. Lee, S. Lim, Y. Jhon, Opt. Fiber Technol. **18**, 112 (2012).

[35] G. Pendock, D. Sampson, Journal of Lightwave Technology **14**(10), 2141 (1996).

[36] A. A. Salman, G. B. Esmer, M. H. Ali, Journal of Optics **53**, 538 (2023).

[37] P. Ravesh, A. Sharma, G Kaur, Opt. Quantum Electronics **54**, 87 (2022).

_____
[*]Corresponding author: Anuragh2468@gmail.com